

93-32  
104 989  
p-10

N92-29377

# Optimizing the $G/T$ Ratio of the DSS-13 34-Meter Beam-Waveguide Antenna

M. S. Esquivel

Ground Antennas and Facilities Engineering Section

*Calculations using Physical Optics computer software were done to optimize the gain-to-noise-temperature ( $G/T$ ) ratio of DSS 13, the DSN's 34-m beam-waveguide antenna, at X-band for operation with the ultra-low-noise amplifier maser system. A better  $G/T$  value was obtained by using a 24.2-dB far-field-gain smooth-wall dual-mode horn than by using the standard X-band 22.5-dB-gain corrugated horn.*

## I. Introduction

During Phase-I testing of the DSS-13 beam-waveguide (BWG) antenna, it was discovered that there was higher system noise temperature than expected. The high noise temperature was caused by the spillover losses of the BWG mirrors having a bigger effect than previously thought. It was experimentally determined that higher-gain horns would improve the  $G/T$  ratio of the antenna because of two reasons: (1) there would be a lower spillover loss in the BWG mirrors and, hence, less noise temperature, and (2) it was hoped that by using higher-gain horns the antenna gain would not decrease significantly.

The Physical Optics (PO) software was used to analyze the theoretical performance of the DSS-13 BWG antenna using three different horn patterns as inputs. The three patterns used were those of corrugated horns with far-field gains of 22.5 dB, 24.2 dB, and 26.1 dB. Each horn pattern was placed at different positions along the z-axis from  $F_3$ , the folded focal point of the basement ellipsoid (see Fig. 1). From the PO analysis, the spillover of the BWG mirrors and the gain of the DSS-13 BWG antenna

could be obtained and, in this manner, various  $G/T$  values could be calculated. All of these calculations were done at 8.45 GHz.

This article presents the results of these calculations. These results were the basis on which a horn was designed to be used in the DSS-13 BWG antenna along with the ultra-low-noise amplifier (ULNA) X-band package. The final design chosen was that of a smooth-wall dual-mode (Potter) horn with a far-field gain of 24.2 dB.

## II. Theoretical Calculations

### A. Method

The theoretical horn patterns mentioned previously were calculated by using software that analyzes a circular waveguide device and computes the  $TE_{mn}$  and  $TM_{mn}$  modes at its ports.<sup>1</sup> The  $TE_{mn}$  and  $TM_{mn}$  modes at the

<sup>1</sup>D. Hoppe, *Scattering Matrix Program for Circular Waveguide Junctions* (internal document), Jet Propulsion Laboratory, Pasadena, California, March 9, 1987.

aperture of a horn are then used to compute the equivalent current distribution. The far-field pattern was calculated using the radiation integral formula. In this case, the standard JPL X-band corrugated horn with a 22.5-dB gain was modeled and its theoretical far-field pattern was computed. The pattern was then converted into a set of spherical wave expansion (SWE) coefficients using software created at JPL by Art Ludwig in the late 1960s [1]. The SWE coefficients were then used as the input to the PO software to obtain the gain of the antenna and the spillover of the BWG mirrors. The method used here was similar to the one used by the designers of the DSS-13 BWG antenna [2].

Besides the 22.5-dB-gain horn, two other corrugated horns (with far-field gains of 24.2 dB and 26.1 dB) were also modeled. These horns were created by simply adding extensions with the same flare angle to the existing 22.5-dB horn circular waveguide configuration geometry. Each of these horns then went through the same process described in the preceding paragraph.

To find the best focus position, each horn aperture was displaced by increments of  $2\lambda$  ( $\lambda = 3.55$  cm) from focal point  $F_3$  in a direction that would bring it closer to mirror  $M_6$  (along the  $+z$ -axis of Fig. 1). By doing this, the spillover was found to decrease and the directivity of the DSS-13 BWG antenna was found to increase slightly. This result in itself was surprising; the phase center of the feed as located in this system was not where expected from previous Phase-I design considerations.

The following formula, Eq. (1), was used to compute the total noise temperature from all the noise contributors:

$$N_t = \sum_{i=1}^M (T_{f_{act}})_i (P_s)_i \quad (1)$$

where  $N_t$  is the total noise temperature (K),  $(T_{f_{act}})_i$  is the temperature factor of the  $i$ th noise contributor (K),  $(P_s)_i$  is the power factor of the  $i$ th spillover contributor, and  $M$  is the number of contributors.

For the DSS-13 BWG antenna, four noise contributors ( $M = 4$ ) are identifiable as follows:

- (1) BWG mirrors (see Table 4)<sup>2</sup>:

- (a) Two lower BWG mirrors with  $(T_{f_{act}})_1$  equal to 300 K.
- (b) Four upper BWG mirrors with  $(T_{f_{act}})_2$  equal to 270 K.
- (2) The subreflector with  $(T_{f_{act}})_3$  equal to 5 K.<sup>3</sup>
- (3) The 34-m main reflector with  $(T_{f_{act}})_4$  equal to 240 K.

Note that the calculations done in this article are applicable to the antenna pointing at the zenith.

The quantity  $(P_s)_i$  in Eq. (1) is directly related to the spillover of each noise contributor by the formula in Eq. (2):

$$(P_s)_i = 1 - 10^{(S_p)_i/10} \quad (2)$$

where  $(S_p)_i$  is the spillover in decibels of each noise contributor computed by the PO software.

## B. Results

After the above calculations were done, the results were plotted in Figs. 2(a)–2(c). Fig. 2(a) shows the efficiency of the DSS-13 BWG antenna for various horns as a function of the horn aperture position measured from  $F_3$  (see Fig. 1). The efficiency plotted in Fig. 2(a) includes the BWG spillover losses and the other losses associated with the antenna as listed in Table 1. For example, the PO software predicts a gain of 68.933 dB for the 22.5-dB corrugated horn with its aperture located  $2\lambda$  from  $F_3$ . This gain corresponds to an efficiency of 86.36-percent at  $f = 8.45$  GHz (69.57 dB is equivalent to 100 percent). The 86.36-percent efficiency would then be placed in the “PO calculation” slot of Table 1 and multiplied by the subtotal efficiency (84.6 percent) to give a total efficiency of 73 percent. This result agrees well with the measured value of 72.4 percent reported.<sup>4,5</sup>

Figure 2(b) shows the total noise temperature of the DSS-13 BWG antenna due to the ULNA and the feeds as a function of horn aperture position with respect to

<sup>3</sup> D. Bathker and W. Veruttipong, *Excess Noise in BWG Antennas: Results of DSS-13 Shroud Testing and Revised DSS-18 Performance Predictions*, presentation viewgraphs, Jet Propulsion Laboratory, Pasadena, California, July 1991.

<sup>4</sup> D. A. Bathker, W. Veruttipong, T. Y. Otoshi, and P. W. Cramer, Jr., *op. cit.*, p. 9.

<sup>5</sup> M. J. Britcliffe, ed., *DSS-13 Beam Waveguide Antenna Project: Phase I Final Report*, JPL D-8451 (internal document), Jet Propulsion Laboratory, Pasadena, California, p. 5–12, March 1991.

<sup>2</sup> D. A. Bathker, W. Veruttipong, T. Y. Otoshi, and P. W. Cramer, Jr., “Beam-Waveguide Antenna Performance Predictions With Comparisons to Experimental Results,” *IEEE Transactions on Microwave Theory and Techniques, Special Issue: Microwaves in Space*, vol. 40, no. 6, edited by R. Dickinson, to be published in June 1992.

$F_3$ . The total noise temperature was obtained by adding the baseline temperature of 11.054 K (see Table 2) of the ULNA to the contributions of the six BWG mirrors, the subreflector and the 34-m main reflector. As expected, the noise temperature decreases as higher-gain horns are used because they cause less spillover in the BWG mirrors than the lower-gain horns.

For example, for the 22.5-dB corrugated horn with its aperture located  $2\lambda$  (7.1 cm) from  $F_3$ , the PO software predicts a spillover noise temperature of 9.41 K. This value was calculated by taking the spillovers computed by the PO software and using Eqs. (1) and (2). The measured BWG noise temperature of this horn is 8.9 K with the aperture placed about 8.4 cm from  $F_3$ .<sup>6</sup> As expected, the smaller displacement from  $F_3$  gives the bigger noise temperature. The comparisons of antenna efficiency and BWG noise temperature with measured results give confidence that the method (specifically the values chosen for  $(T_{fact})_i$  of the four noise contributors) that is used to do these calculations does work.

Figure 2(c) shows the  $G/T$  values of the DSS-13 BWG antenna for the horns as a function of their aperture position with respect to  $F_3$ . The  $G/T$  ratio is calculated by converting the efficiencies of Fig. 2(a) to decibels and then subtracting the total noise temperature (in decibels).

### III. Horn Selection

Since the purpose of this study is to optimize the  $G/T$  ratio of the DSS-13 BWG antenna, Fig. 2(c) needs to be examined closely to select the proper horn. It seems that a corrugated horn with far-field gain between 24 and 26 dB is the best choice.

Because of cost considerations, it was decided to use an existing JPL design for a 22-dB smooth-wall dual-mode circular horn design instead of a corrugated feed. The smooth-wall dual-mode circular feed is usually referred to as the Potter horn, since P. D. Potter was the original designer [3]. The Potter horn has a smooth-wall flare section 54.193 cm in length with a horn-flare half angle of 6 deg 15 arcmin 15 arcsec. The radius at its aperture is 8.2487 cm.<sup>7</sup> The plan was to add an extension on top of the existing ULNA Potter horn that would give a far-field gain between 24 and 26 dB.

Since the extension was to be built at JPL and there were cost limitations, it was decided to modify the existing

<sup>6</sup> D. Bathker and W. Veruttipong, op. cit.

<sup>7</sup> JPL Assembly Drawing D23835-13696 (internal document), Jet Propulsion Laboratory, Pasadena, California, 1969.

horn to have a far-field gain of 24.2 dB instead of 26 dB. To accomplish this, a 25.4-cm extension (with the same flare angle, input radius = 8.2487 cm and output radius = 11.033 cm) needed to be used. The original Potter horn has a phasing section that is 0.721 cm in length. The purpose of this phasing section is to fix the differential phase between the  $TE_{11}$  and  $TM_{11}$  modes at the aperture of the horn so that an equal beam width pattern is created.

Since a 25.4-cm extension has been added, the  $TE_{11}$  and  $TM_{11}$  will not be properly phased at the aperture. Making use of Eqs. (11) and (12) in [3], the new phasing section needs to be adjusted to a length of 6.48 cm. Figure 3 shows the geometry of this new 24.2-dB Potter horn.

To appreciate the importance of the phasing section, compare Figs. 4(a) and 4(b), which show the far-field patterns for a Potter horn with a 25.4-cm extension and phasing section lengths of 6.48 cm and 0.721 cm, respectively. Notice how the 6.48-cm phasing section gives equal beam widths out to  $\theta = 15$  deg and a 24.2-dB gain while the 0.721-cm phasing section gives a smaller gain (23.8 dB) with unequal beam widths.

The new 24.2-dB Potter horn was then run through the PO software as the other horns were. The results are shown in Figs. 2(a)–2(c), under 24.2-dB Potter horn. Only four cases were run for this horn because results for the corrugated horns predicted that the optimum  $G/T$  ratio would be achieved when the horn aperture-to- $F_3$  displacement was about  $10\lambda$ . Notice that the predicted  $G/T$  ratio for the 24.2-dB Potter horn is better than for all the horns. This is due to the fact that while the antenna efficiency is at the same level as for the 24.2-dB corrugated horn (see Fig. 2(a)), the noise temperature is about 0.7 K lower (see Fig. 2(b)). The noise temperature is less because the PO software predicts that the 24.2-dB Potter horn has nearly the same spillover as the 26.1-dB corrugated horn.

### IV. Experiment

The new 24.2-dB Potter horn was built. Radiation patterns were measured at the JPL mesa antenna-range facility. Since these patterns were recorded on a strip chart, they were visually compared to the theoretical patterns of Fig. 4(a) and were found to be satisfactory. Then, in November 1991, the system noise temperature of the DSS-13 BWG antenna was measured using the 24.2-dB Potter horn with the ULNA. The horn's aperture was placed  $8.61\lambda$  ( $f = 8.45$  GHz) from  $F_3$ . A value of  $N_t = 14.4$  K

was observed.<sup>8</sup> This measured point is shown in Fig. 2(b). The predicted noise temperature for the 24.2-dB Potter horn at  $8.61\lambda$  is 12.78 K. At the present time, reasons for the small differences between the measured and calculated values are being investigated. Further work in this area is warranted.

## V. Conclusions

A method has been developed that can be used to calculate the optimum-gain horn to be used in the DSS-13

---

<sup>8</sup>H. K. Detweiler, JPL Internal Memorandum 3330-92-002 (internal document), Jet Propulsion Laboratory, Pasadena, California, January 7, 1992.

34-m BWG antenna. The ability to predict the total system efficiency of the BWG system using this method was found to be highly accurate and agreed with measurements; however, work needs to be done to improve the noise-temperature prediction model. It was shown that the location of the position of the feed horn had to be modified such that the typical far-field phase center position is not used; rather, a near-field phase center located deeper inside the horn optimizes both the antenna noise temperature and the  $G/T$  ratio. This design was used to fabricate a Potter horn for the X-band ultra-low-noise amplifier maser system that was recently demonstrated at the DSS-13 34-m BWG antenna. The 1.62 K difference in measured and calculated noise temperatures of this demonstration warrants further study.

## Acknowledgments

The author would like to thank the JPL Supercomputing Project for facilitating the use of Voyager, the new CRAY Y-MP2E/116 supercomputer. It would have been impossible to have completed this  $G/T$  ratio optimization study without the numerous CPU hours burned up on this powerful machine.

The noise-temperature models used in this article have been a direct result of the efforts of all the individuals from the JPL Ground Antennas and Facilities Engineering Section who have been a part of the DSS-13 BWG Antenna Project.

Finally, the author acknowledges Mark Gatti for many insightful discussions and for suggesting that this study be undertaken.

## References

- [1] A. C. Ludwig, "Near-Field Far-Field Transformations Using Spherical-Wave Expansions," *IEEE Transactions on Antennas and Propagation*, vol. AP-19, no. 2, pp. 214-220, March 1971.
- [2] T. Veruttipong, W. Imbriale, and D. Bathker, "Design and Performance Analysis of the DSS-13 Beam Waveguide Antenna," *TDA Progress Report 42-101*, vol. January-March 1990, Jet Propulsion Laboratory, Pasadena, California, pp. 99-113, May 15, 1990.
- [3] P. D. Potter, "A New Horn Antenna With Suppressed Sidelobes and Equal Beamwidths," *Microwave Journal*, vol. 6, pp. 71-78, June 1963.

Table 1. DSS-13 BWG antenna: overall gain accounting X-band at  $F_3$ .<sup>a</sup>

Element	Efficiency, percent	Notes
Main reflector:		
$I^2R$	0.99954	
Panel leakage	0.99992	
Gap leakage	0.9982	
RMS	0.977	Normal 0.45 mm (0.0177 in.)
Subreflector:		
$I^2R$	0.99954	
RMS	0.998	Normal 0.125 mm (0.005 in.)
Four BWG mirrors:		
$I^2R$	0.99807	
RMS	0.996	Each normal 0.125 mm (0.005 in.)
Two BWG mirrors:		
$I^2R$	0.99903	
RMS	0.997	Each normal 0.125 mm (0.005 in.)
BWG/Cassegrain VSWR	0.999	Estimated
Waveguide:		
$I^2R$	0.984	Loss = -0.070 dB
VSWR	0.99	
Feed support blockage	0.918	X-band, tripod, 2.7%, 1.55 factor
Bypass blockage	0.987	9-ft equivalent diameter
Pointing squint	0.9954	Scan loss = -0.02 dB
Mirror alignments	0.9994	Based on 0.99 at 32 GHz
Subtotal:	0.844491	
PO calculation	Variable	Includes BWG mirrors' spillover losses. Dependent on horn gain and position
Total efficiency	Variable	69.573 dB is 100% at 8.45 GHz. Dependent on horn gain and position

<sup>a</sup>This table is based on D. A. Bathker, W. Verruttipong, T. Y. Otoshi, and P. W. Cramer, Jr., op. cit., p. 21.

**Table 2. DSS-13 BWG antenna: overall noise accounting X-band at  $F_3$  at 90-deg elevation.<sup>a</sup>**

Element	Noise, K	Notes
Cosmic background	2.5	Equivalent blackbody
Atmosphere	2.17	Goldstone (average clear) <sup>b</sup>
Four mirror $I^2R$ /BWG	0.572	
Two mirror $I^2R$ /BWG	0.272	
Main reflector:		
$I^2R$	0.136	
Panel leakage	0.02	
Gap leakage	0.5	
Subreflector:		
$I^2R$	0.134	
Tripod scatter	2	
Bypass scatter	0.07	
Subtotal	8.374	
ULNA	2.68	Based on roof measurements of ULNA and the new horn <sup>c</sup>
Baseline (ULNA plus subtotal)	11.054	
DSS-13 spillover:		
Two lower BWG mirrors	Variable	$T_{fact} = 300$ K
Four upper BWG mirrors	Variable	$T_{fact} = 270$ K
Subreflector	Variable	$T_{fact} = 5$ K
Main reflector	Variable	$T_{fact} = 240$ K
Total noise	Variable	Depends on horn gain and aperture position

<sup>a</sup> This table is based on D. A. Bathker, W. Verruttipong, T. Y. Otoshi, and P. W. Cramer, Jr., op. cit., p. 23.

<sup>b</sup> S. D. Slobin, "Atmospheric and Environmental Effects," Module TCI-40, Rev. C, *DSN/Flight Project Interface Design*, Document 810-5, Rev. D (internal document), Jet Propulsion Laboratory, Pasadena, California, 1991.

<sup>c</sup> M. Gatti, Manager, DSS-13 Beam-Waveguide Antenna Project, personal communication, Jet Propulsion Laboratory, Pasadena, California, January 1992.

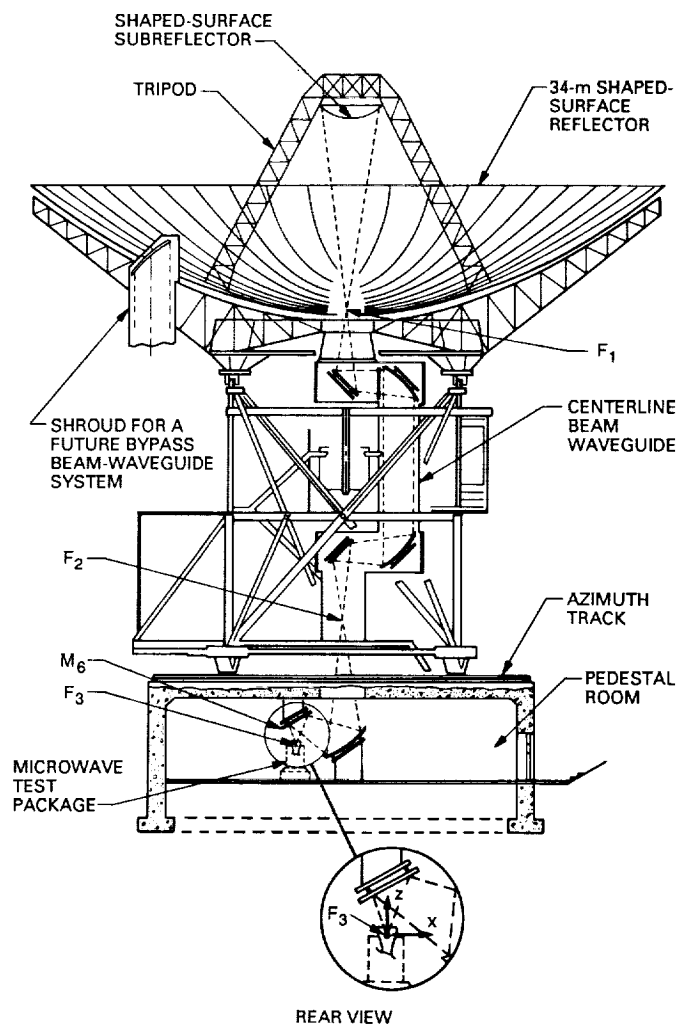


Fig. 1. Configuration of DSS-13 antenna.

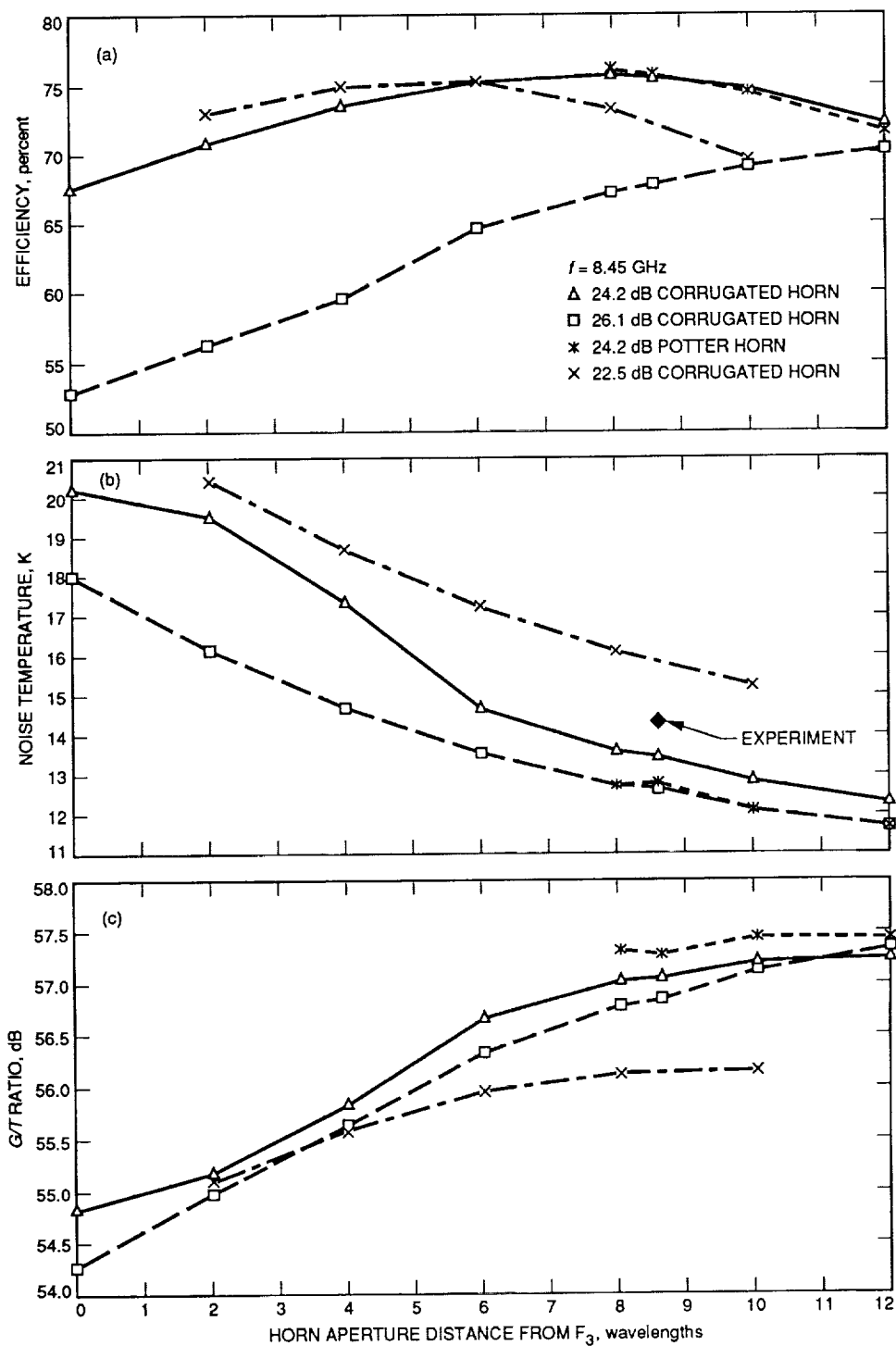


Fig. 2. DSS 13: (a) efficiency versus horn aperture distance from F<sub>3</sub>; (b) system temperature versus horn aperture distance from F<sub>3</sub>; and (c) G/T ratio versus horn aperture distance from F<sub>3</sub>.



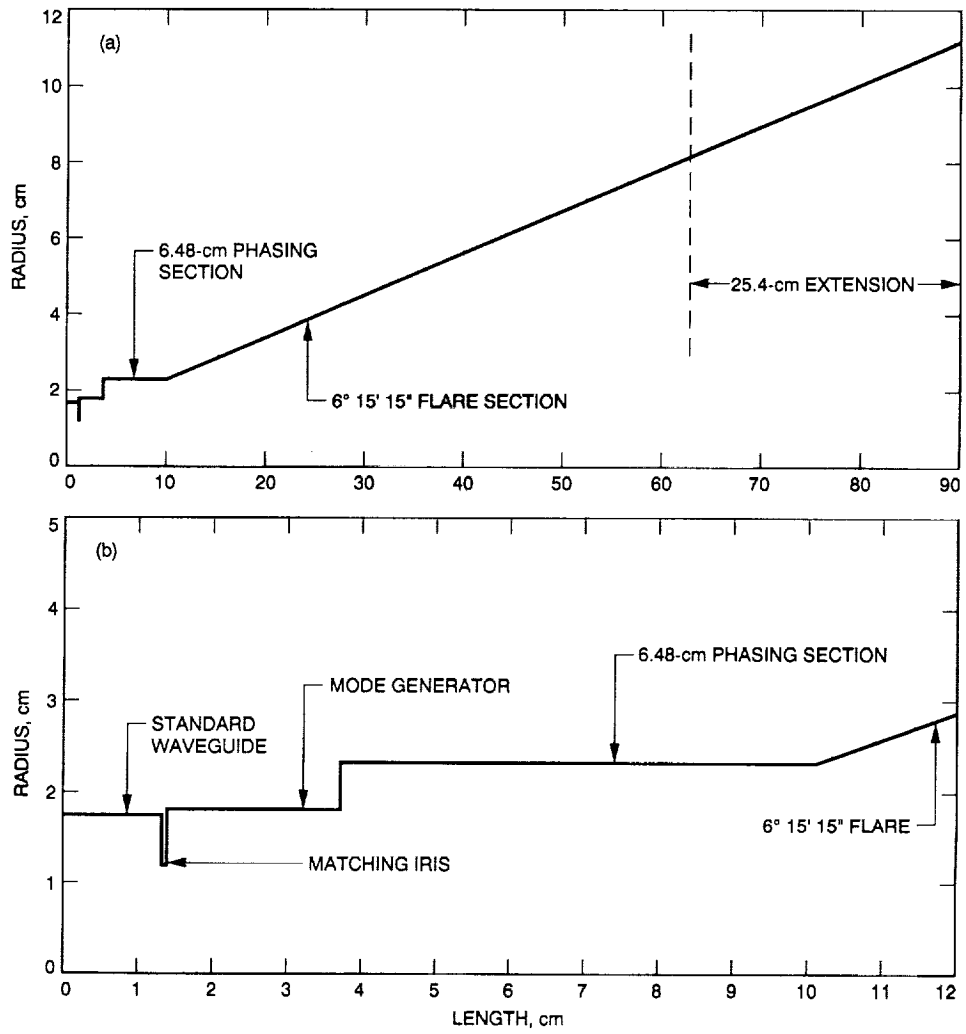


Fig. 3. X-band 24.2-dB Potter horn dimensions: (a) overall feed and (b) input section.

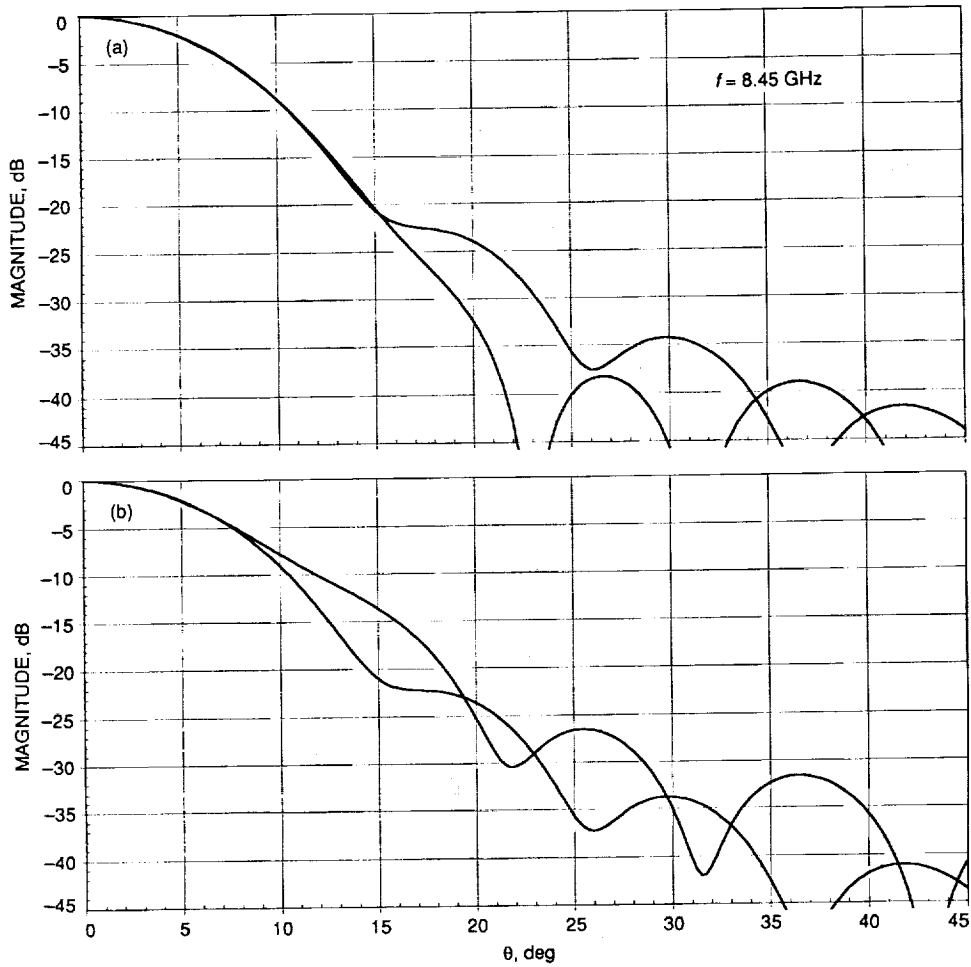


Fig. 4. X-band radiation patterns of the Potter horn with: (a) 24.2-dB gain: 6.48-cm phasing section and (b) 23.8-dB gain: 0.721-cm phasing section.